

## Investigating the Effect of Thymol Active Ingredient and ZnO Nanoparticle Conjugated by Thiosemicarbazone on the Expression of Efflux Pump and Biofilm Genes in *Pseudomonas aeruginosa*

Hadiseh Mokhtari, Seyedeh Tooba Shafighi\*, Ali Salehzadeh\*, Somayeh Ataei jaliseh

Department of Biology, Rasht Branch, Islamic Azad University, Rasht, Iran

### ARTICLE INFO

#### Article history:

Received 24 September 2022

Accepted 01 November 2022

Available online 22 January 2023

#### Keywords:

Biofilm

Efflux pump

Quantitative PCR

Thiosemicarbazone

Zinc oxide

#### \*Corresponding authors:

✉ T Shafighi

tshafighi@yahoo.com

✉ A Salehzadeh

salehzadeh@iaurasht.ac.ir

p-ISSN 2423-4257

e-ISSN 2588-2589

### ABSTRACT

Finding novel antimicrobials to treat drug-resistant *Pseudomonas aeruginosa* is a major health challenge. In this study, ZnO nanoparticles functionalized by Thiosemicarbazone nanoparticles (ZnO@Glu-TSC NPs) were synthesized and the effect of the NPs alone and in combination with thymol on the expression of biofilm and efflux pump genes in *P. aeruginosa* was investigated. Physicochemical features of the ZnO@Glu-TSC NPs were evaluated by FT-IR, XRD, EDS-mapping, and SEM and TEM imaging. The inhibitory effect of ZnO@Glu-TSC NPs and thymol, alone and in combination, were determined by broth microdilution method, and quantitative PCR was used to evaluate the expression of the *pelA*, *pslA*, *algD*, *mexA*, *mexB*, and *mexX* genes. The synthesized NPs were almost spherical, without impurities, and in a size range of 20 to 60 nm. Simultaneous treatment of *P. aeruginosa* with ZnO@Glu-TSC and thymol had a significantly stronger inhibitory effect (MIC: 3.12-25.5 µg/mL) than either agent alone. The relative expression of the *pelA*, *pslA*, and *algD* genes in *P. aeruginosa* strains treated with ZnO@Glu-TSC+thymol was reduced by 0.44, 0.43, and 0.46 folds, respectively. Furthermore, the expression of *mexA*, *mexB*, and *mexX* genes decreased in *P. aeruginosa* strains treated with ZnO@Glu-TSC+thymol (0.42, 0.45, and 0.41 folds, respectively). Also, it was found that the combination of ZnO@Glu-TSC and thymol could synergistically reduce the expression of the mentioned genes in comparison with either agent alone. This study showed that ZnO@Glu-TSC NPs and thymol synergistically inhibited biofilm maturation and efflux pump systems in *P. aeruginosa* strains and could be considered a novel antibacterial candidate against *P. aeruginosa* strains.

© 2023 University of Mazandaran

**Please cite this paper as:** H Mokhtari, T Shafighi, Ali Salehzadeh, S Ataei-e jaliseh. 2023. Investigation of the effect of thymol active ingredient and zno nanoparticle conjugated by thiosemicarbazone on the expression of efflux pump and biofilm genes in *Pseudomonas aeruginosa*. *J Genet Resour* 9(1): 75-82. doi: 10.22080/jgr.2023.24604.1338

### Introduction

*Pseudomonas aeruginosa* is a gram-negative bacterium that is an opportunistic human pathogen responsible for several nosocomial and community-acquired infections (Tuon *et al.*, 2022; Dai *et al.*, 2019). This bacterium can adapt to environmental changes, develop antibacterial resistance, and produce a large number of virulence factors (Tuon *et al.*, 2022). *P. aeruginosa* could develop life-threatening infections, especially in burns, cystic fibrosis,

and immunocompromised patients. In addition to the virulence factors, the development of antibiotic resistance is a major cause of infection progression and therapeutic failure of *P. aeruginosa* infections. The emergence of drug resistance is an important challenge in treating *P. aeruginosa* strains. Therefore, many studies aim to find novel antimicrobials to combat *P. aeruginosa* infections. Biofilm formation and active extrusion of antibacterial drugs by bacterial efflux systems play a major role in the



antibiotic resistance of this bacterium (Tuon *et al.*, 2022; Dai *et al.*, 2019). Biofilm is a bacterial community adhering to a surface and embedded in self-produced extracellular polysaccharide substances (EPS), including polysaccharides, proteins, and DNA molecules (Ha and O'Toole, 2015). It has been reported that bacteria in biofilm growth show considerably more resistance to antibacterial substances (up to 1000 folds). The decreased susceptibility to antibiotics is related to the physical protection of bacterial cells from the drugs by bacterial EPS, and the lower metabolic and growth rate of bacterial biofilm compared to planktonic growth (Ha and O'Toole, 2015; Franklin *et al.*, 2011). Extracellular polysaccharides including alginate, Pellicle polysaccharide (Pel), and Pentasaccharide repeating units (Psl) are considered the major components of the *P. aeruginosa* biofilm matrix.

Alginate is a high molecular weight polysaccharide composed of O-acetylated d-mannuronic acid that is secreted into the surrounding medium and results in highly viscous colonies (Franklin *et al.*, 2011). The Psl is a repeating pentamer polysaccharide composed of d-mannose, l-rhamnose, and d-glucose and facilitates cell-cell and cell-surface interactions during biofilm development (Ma *et al.*, 2009). It was reported that Psl provides a fabric-like matrix that provides cell-to-cell connection in the biofilm matrix. Pel seems to be a glucose-rich polysaccharide that plays a role in cell-to-cell connection and the formation of a structured pellicle at the air-liquid interface in *P. aeruginosa* biofilm (Coulon *et al.*, 2010).

*P. aeruginosa* employs several efflux systems to extrude antimicrobial drugs from bacterial cytoplasm to the extracellular environment, which reduces the accessibility of the antibiotics to their target sites. Two efflux systems, including mexAB-oprM and mexXY-oprM, are considered the most important efflux systems responsible for the resistance to a large number of antimicrobial agents (Dreier *et al.*, 2010).

Thymol (2-isopropyl-5-methyl phenol) is an essential oil that is naturally isolated from the thyme or Lamiaceae family plants with several biological properties, including antibacterial, antifungal, antibiofilm, and antioxidant activities (Kazemi - Pasarvi *et al.*, 2020; Najafloo *et al.*,

2020). Previous studies showed that the simultaneous use of Thymol with metal nanoparticles (NPs) not only can increase their antibacterial potential but also may reduce the undesirable cytotoxic effects of the NPs (Kazemi - Pasarvi *et al.*, 2020). Given the small size, NPs have a large effective surface that could provide novel characteristics to be used in biomedical applications. Nano-sized ZnO and its derivatives have shown considerable antibacterial potential over a wide spectrum of bacteria (Sirelkhatim *et al.*, 2015). Several mechanisms are associated with the antibacterial property of ZnO NPs, including the destruction of bacterial cell integrity through direct contact with the bacterial cell wall, the liberation of Zn<sup>2+</sup> antimicrobial ions, and the generation of reactive oxygen species (ROS) that results in the damage to cell components (Sirelkhatim *et al.*, 2015; Li *et al.*, 2011).

Thiosemicarbazone is a chemical compound with several biomedical properties such as antibacterial, antifungal, and anticancer activities (Tada *et al.*, 2011). The antibacterial activity of TSC mainly relies on the chelation of essential ions from the bacterial surface that damage the bacterial envelope (Nejabatdoust *et al.*, 2019). Therefore, ZnO@Glu-TSC NPs could provide a considerable antibacterial activity that is reported in the literature (Nejabatdoust *et al.*, 2019).

In this regard, the present study investigated the effect of treating *P. aeruginosa* strains with Thymol and ZnO nanoparticle functionalized by Thiosemicarbazone (ZnO@Glu-TSC) on the expression of some alginate, Pel, Psl, and efflux pump genes.

## Materials and Methods

### Synthesis of ZnO@TSC NPs

At first, the ZnO@Glu NPs were synthesized using a method described previously (Nejabatdoust *et al.*, 2020). In brief, a mixture containing 20mL of 0.1 M ammonia solution, 0.5M ZnCl<sub>2</sub>.6H<sub>2</sub>O solution, and glutamic acid (with a 1:2 mole ratio) was prepared and heated at 100°C for 60 min. Next, the generated ZnO NPs were separated, washed (with distilled water and ethanol), and dried at 80°C for 8 h. To conjugate TSC to ZnO@Glu NPs, 500mg of ZnO@Glu and 200 mg of TSC (Merck,

Germany) were sonicated in 100mL ethanol for 30 min and then stirred overnight at 40°C. Finally, the ZnO@Glu-TSC was harvested by centrifugation, washed with water and ethanol, and dried at 60°C for 6 h.

### Characteristics of ZnO@Glu-TSC NPs

Physicochemical characteristics of ZnO@Glu-TSC NPs were studied using Fourier-transform infrared (FT-IR) spectroscopy, X-ray crystallography (XRD), Scanning and Transmission electron microscopy (SEM and TEM), and Energy dispersive spectrometry (EDS) analyses. The FT-IR (Perkin-Elmer FT-IR spectrophotometer 100) and XRD (Philips, PW1730) were used to evaluate the functional groups and crystalline structure of the NPs, respectively. SEM (TESCAN Mira3) and TEM (Zeiss EM-900) imaging were also used to determine the particle size, morphology, and distribution of the NPs. Moreover, an EDS-mapping analysis was used to evaluate the elemental composition of ZnO@Glu-TSC NPs (TESCAN Mira3).

### Bacterial strains

A total number of *P. aeruginosa* strains, including three pathogenic strains and reference *P. aeruginosa* (ATCC 19429) were used in this work. Pathogenic *P. aeruginosa* strains were received from the clinical samples (injuries and urine) from infected patients (Rasht, Iran) and identified using gram staining, culture in selective media, and standard biochemical assays.

### Minimum inhibitory concentration

The Minimum inhibitory concentration (MIC) of the ZnO@Glu-TSC NPs and thymol for *P. aeruginosa* strains were measured by preparing a serial dilution of the NPs and thymol (3.125-100 µg/mL) in 96-well plates. Initially, the NPs and thymol were dissolved as stock solutions (100 mg/mL) in dimethylsulfoxide (DMSO) and diluted in Mueller-Hinton broth. Then, 100 µL of a fresh bacterial suspension was added to the wells and the plates were incubated overnight at 37°. The minimum concentration of each compound that inhibited bacterial growth was regarded as MIC (Nejabatdoust *et al.*, 2020).

### Treating *P. aeruginosa* with ZnO@Glu-TSC NPs and thymol

After measuring the MIC of each agent, a fresh culture of *P. aeruginosa* strains was prepared in Tryptic soy broth and treated with the NPs and thymol at their sub-inhibitory concentration. A total number of four experimental groups were designed, including a) treating bacterial cells with ZnO@Glu-TSC NPs, b) treating bacterial cells with thymol, c) treating bacterial cells with ZnO@Glu-TSC NPs and thymol, and d) control cultures. After incubation for 8 h at 37 °C, bacterial cells were harvested by centrifugation.

### Gene expression

The harvested bacteria were subjected to RNA extraction using the TriZol™ (Thermo Fisher, USA) RNA extraction kit, according to the manufacturer's instructions. The extracted RNA samples were treated with DNaseI (Cinaclone, Iran) to remove their DNA content. Then, the quality and quantity of RNA samples were evaluated by agarose gel electrophoresis and nanodrop spectrophotometry. The cDNA molecules were synthesized by the Yekta Tajhiz cDNA Synthesis Kit (Iran), according to the instruction.

The relative expression of six *P. aeruginosa* virulence genes, the genes responsible for bacterial biofilm and efflux pumps were studied using the SYBR Green quantitative PCR assay (QIAGEN, Germany). The studied genes were as follows: *pslA*, *pelA*, *algD*, *mexA*, *mexB*, and *mexX*. Also, the *16s rRNA* gene was used as an internal control gene (in three replicates). The characteristics of the primers used in this study are presented in Table 1. The assay was performed in three technical replicates and the expression of each gene in treated cells (relative to their respective control) was determined by the  $2^{-\Delta\Delta Ct}$  method (Pfaffl, 2001).

### Statistical analysis

The statistical difference between the treatment groups was analyzed by the SPSS. 16.0 software, using *one-way ANOVA* analysis and considering the p-values of less than 0.05 statistically significant.

**Table 1.** The sequence of the primers used in this study.

Primer	Sequence (5'→ 3')	Amplicon size	Reference
pelA-F	5'-GGTATCTGAAAGAGCAGG	190	[This research]
pelA-R	5'-GTAGCCCTGTTTGCGCAGCTC		
algD-F	5'-CTGATCAACCAGGGCAAGTCG	135	[This research]
algD-R	5'-GCTCGGCGTGCCGACGCAGAT		
pslA-F	5'-ATGTTCCAGGCACTGGACGTC	147	[This research]
pslA-R	5'-CCAGAAGATCACCAGCTTGCT		
mexA-F	5'-AAGCGCCTGTTCAAGGAAGGC	175	[This research]
mexA-R	5'-GGACTGCAGGTAGGCGGCATT		
mexB-F	5'-TTCATTGATAGGCCATTTTC	200	[This research]
mexB-R	5'-GATGTAGCGCAGATTGTCGAT		
mexX-F	5'-AGTGCTGTTCCAGATCGAC	140	[This research]
mexX-R	5'-GGTGTACTCGCGTTCGCTGAT		
16S rRNA-F	5'-GGGACCCGCACAAGCGGTGG-3'	191	[Atshan <i>et al.</i> , 2013]
16S rRNA-R	5'-GGGTTGCGCTCGTTGCGGGA-3'		

## Results

### Characteristics of the ZnO@Glu-TSC NPs

The FT-IR assay was used to evaluate the functional groups of the ZnO@Glu and ZnO@Glu-TSC NPs. According to the spectrogram of ZnO@Glu, the peaks observed at 638 and 712  $\text{cm}^{-1}$  are related to the vibration of Zn-O and C-H bonds, respectively. Additionally, the peaks observed at 885 and 1100  $\text{cm}^{-1}$  belong to the C-O and C=O bonds. Moreover, the C-C, C=N, and N-H bonds caused peaks at 1368, 1467, and 1550  $\text{cm}^{-1}$ . The absorption peak that appeared at 3634  $\text{cm}^{-1}$  is associated with the scattering O-H bond.

The FT-IR spectrogram of ZnO@Glu-TSC NPs showed the peaks associated with the Zn-O, C-H, C-O, S=O, and N-O bonds at 648, 783.4, 1000.3, and 1368  $\text{cm}^{-1}$ , respectively. Also, the peaks at 1627.24, 2010, 1589.3, and 2641.3 are related to the C=N, N=H, C-N, and N-N bonds, respectively. Finally, the peaks observed at 3000-4000  $\text{cm}^{-1}$  could be associated with the O-H bond (Fig. 1).

The XRD analysis was used to evaluate the crystalline structure of the ZnO@Glu-SC NPs. According to the XRD pattern, the peaks were observed at 2 $\theta$  of about 31.9, 34.5, 36.3, 47.6, 56.7, and 62.9 degrees that comply with the JCPDS card No.89-1397 (Foo *et al.*, 2014; Khan *et al.*, 2016). The peaks at 2 $\theta$  of 10-30 degrees could be related to the Glutamic acid and considering the amorphous nature of TSC, the peak observed at 2 $\theta$  of 29.8 suggests the presence of TSC molecules (Fig. 2).

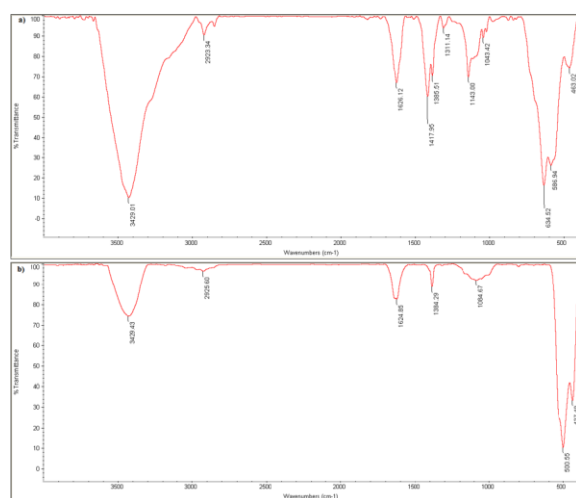


**Fig. 1.** FT-IR analysis: a) ZnO@Glu; b) ZnO@Glu-TSC NPs. The peaks associated with the Zn-O, C-H, C-O, S=O, and N-O bonds are at 648, 783.4, 1000.3, and 1368  $\text{cm}^{-1}$ , respectively.

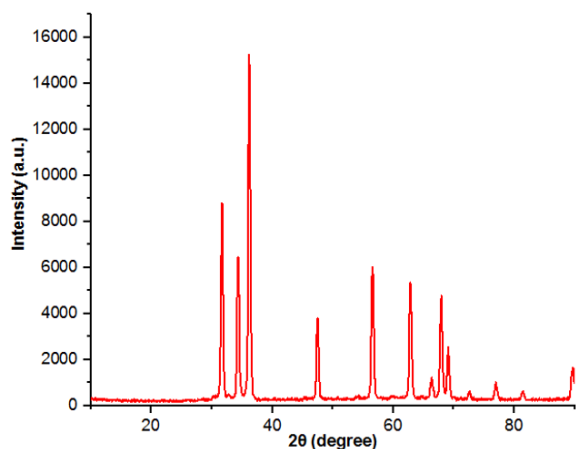


**Fig. 2.** XRD pattern of ZnO@Glu-TSC NP. According to the XRD analysis, the peaks at 31.9, 34.5, 36.3, 47.6, 56.7, and 62.9 degrees correspond to crystal structure of ZnO NP.

The SEM and TEM imaging of the ZnO@Glu-TSC showed that the NPs were almost spherical, with low aggregation, and were in a size range of 20 and 60 nm (Fig. 3).

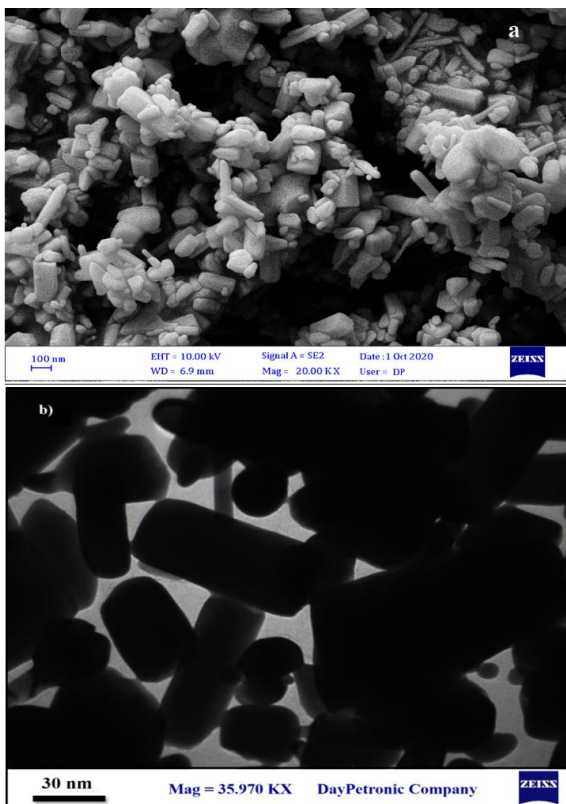


**Fig. 3.** Electron microscope images of the synthesized ZnO@Glu-TSC NPs: A) SEM; B) TEM. The size range of ZnO@Glu-TSC NPs are from 20 to 60 nm.

Investigation of the elemental composition of ZnO@Glu-TSC showed that the synthesized NPs contained C, N, O, S, and Zn atoms that indicate the purity of the NPs. The EDS-mapping of the ZnO@Glu-TSC NPs is presented in the Fig. 4.

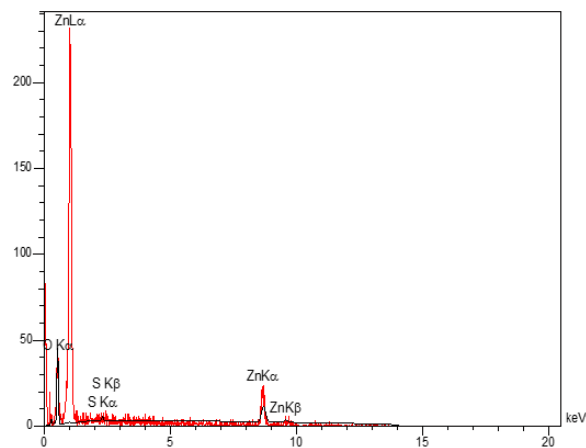


**Fig. 4.** EDS-mapping analysis of ZnO@Glu-TSC NPs. The figure shows that the C, N, O, S, and Zn elements are present in the composition of ZnO@Glu-TSC NP.

Investigating the effect of ZnO@Glu-TSC and thymol alone or in combination on the expression of biofilm-associated genes showed that the studied agents reduced the expression of *pslA*, *pelA*, and *algD* genes. Treating pathogenic and ATCC *P. aeruginosa* strains with ZnO@Glu-TSC decreased the expression of *pslA* by 0.37 and 0.30 folds, respectively. Additionally, the expression of this gene was reduced by 0.17-0.27 folds among the strains treated with thymol. Simultaneous treatment of bacterial cells with ZnO@Glu-TSC, and thymol reduced the expression of *pslA* by 0.38-0.44 folds. Similarly, the expression of *pelA* in ZnO@Glu-TSC and thymol-treated bacteria decreased by 0.37 and 0.25 folds, respectively. Moreover, ZnO@Glu-TSC+ thymol (in combination) decreased the *pelA* by 0.44 folds. Treating *P. aeruginosa* strains with ZnO@Glu-TSC, thymol, and ZnO@Glu-TSC+thymol also reduced the expression of *algD* by 0.40, 0.23, and 0.46 folds, respectively (Fig. 5).

**Table 2.** The minimum inhibitory concentration of different agents on *P. aeruginosa* strains.

Minimum inhibitory concentration (µg/mL)			
Strain	Thymol	ZnO@Glu-TSC	Thymol+ ZnO@Glu-TSC
PA-19	25	12.5	6.25
PA-26	50	25	12.5
PA-27	25	12.5	3.125
PA-ATCC19429	50	50	25.5

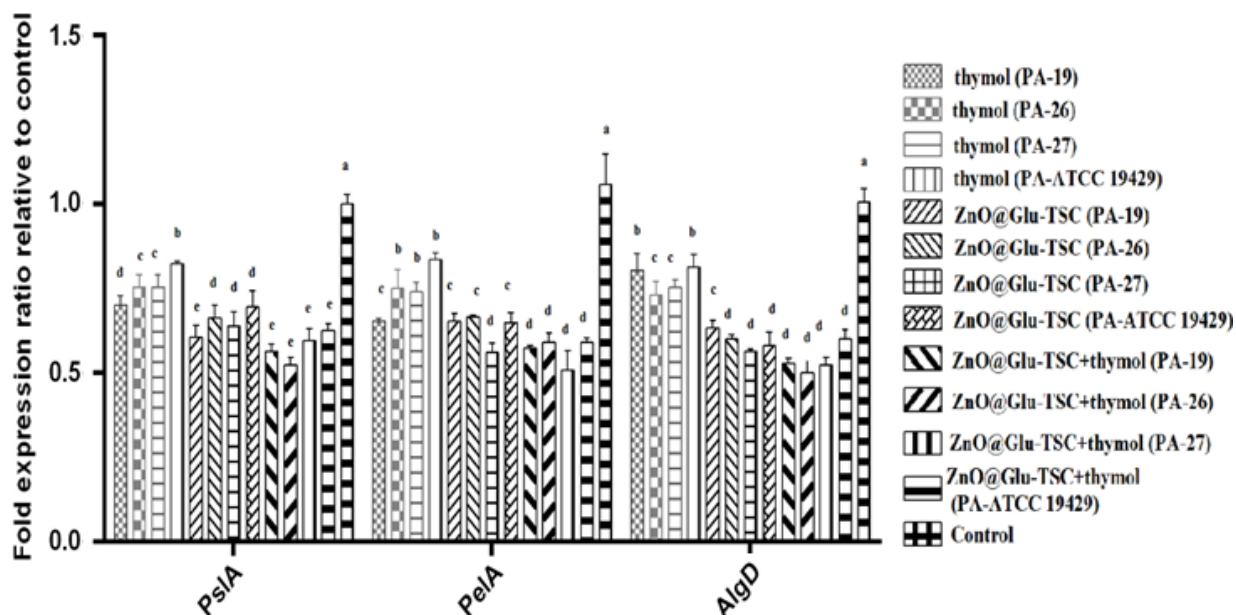


**Fig. 5.** The effect of thymol, ZnO@Glu-TSC NPs, and thymol+ ZnO@Glu-TSC NPs on the expression of *P. aeruginosa* biofilm-related genes. Different letters show significant differences ( $p < 0.5$ ).

Evaluating the effect of ZnO@Glu-TSC and thymol alone and in combination on the expression of efflux pump genes- *mexA*, *mexB*, and *mexX*- revealed that the expression of all genes was significantly decreased. According to the results, the highest reduction of the *mexA* was observed among the cells treated with ZnO@Glu-TSC+thymol (0.33-0.47 folds), followed by the cells treated with ZnO@Glu-TSC alone (0.26-0.39 folds). A similar pattern

was observed for the *mexB* gene, which was reduced by 0.35, 0.22, and 0.44 folds among the strains treated with ZnO @ Glu-TSC, thymol, and ZnO @ Glu-TSC + thymol, respectively. Investigating the expression of the *mexX* in treated cells showed similar results with the reduction of 0.32, 0.20, and 0.40 in ZnO@Glu-TSC, thymol, and ZnO@Glu-TSC+thymol treated cells (Fig. 6).

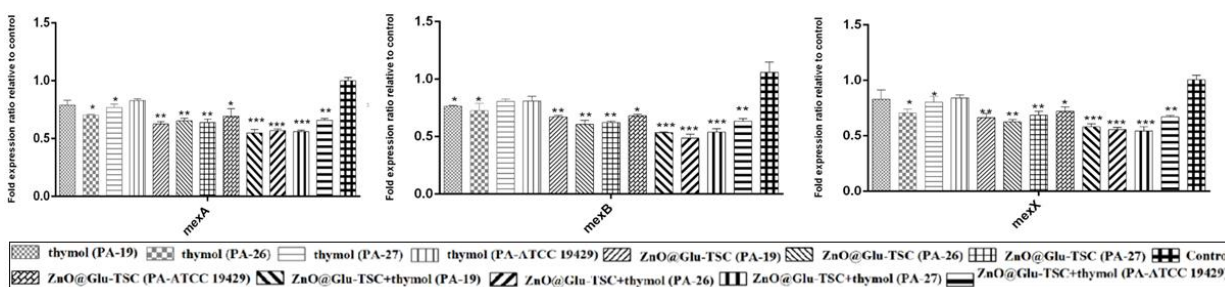


**Fig. 6.** The effect of thymol, ZnO@Glu-TSC NPs, and thymol+ ZnO@Glu-TSC NPs on the expression of *mex* genes in *P. aeruginosa* strains.

## Discussion

Thymol has shown efficient antibacterial activity over a large number of bacteria, including gram-positive and gram-negative species (Najafloo *et al.*, 2020). The antibacterial activity of thymol relies on the inhibition of bacterial ATP generation and damage to the cell envelope that results in the leakage of cytoplasm components (Najafloo *et al.*, 2020). The synergism of thymol with ZnO NPs has been previously reported in the literature (Kazemi - Pasarvi *et al.*, 2020; Yanishlieva *et al.*, 1999). Evaluation of the inhibitory effect of thymol and ZnO@Glu-TSC NPs for *P. aeruginosa* strains showed that both agents have considerable antibacterial properties. However, simultaneous treatment of *P. aeruginosa* showed considerable synergism of ZnO@Glu-TSC NPs and thymol that decreased the MIC value.

Based on the results of the current study, it was found that ZnO@Glu-TSC NPs and thymol alone or in combination can significantly decrease the expression of the genes responsible for bacterial extracellular polysaccharides. Pel, Psl, and alginate play critical roles in biofilm development and maturation (Franklin *et al.*, 2011; Coulon *et al.*, 2010). Therefore, the considerable reduction of the *pelA*, *pslA*, and *algD* showed that ZnO@Glu-TSC NPs and thymol might synergistically inhibit bacterial biofilm, which could increase the susceptibility of *P. aeruginosa* to either agent.

Similarly, it was observed that the simultaneous treatment of *P. aeruginosa* with ZnO@Glu-TSC NPs and thymol inhibited the expression of the *mexA*, *mexB*, and *mexX* genes. The MexA and MexX are bacterial periplasmic lipoproteins that play important roles in the extrusion of antibiotics from bacterial cytoplasm. In addition, MexB is a membrane-bound protein that delivers antimicrobial agents to its periplasmic counterpart of the efflux pump (Askoura *et al.*, 2011). Synergic reduction of all studied efflux pump genes also revealed that the major efflux systems MexAB-OprM and MexXY-OprM of *P. aeruginosa* were inhibited and failed to extrude ZnO@Glu-TSC NPs and thymol from bacterial cytoplasm, which resulted in the damages to the intracellular components of bacterial cells. However, further investigations are required to determine the possible

mechanism of efflux pump inhibition by ZnO@Glu-TSC NPs and thymol.

## Conclusion

According to the findings, it was found that ZnO@Glu-TSC NPs and thymol could synergistically reduce the expression of the *pslA*, *pelA*, *algD*, *mexA*, *mexB*, and *mexX* genes, which could significantly reduce bacterial virulence and drug resistance.

## Conflict of interests

The authors declare no conflicts of interest.

## References

- Atshan SS, Shamsudin MN, Karunanidhi A., van Belkum A, Lung LTT, Sekawi Z, ..., Abduljaleel SA, 2013. Quantitative PCR analysis of genes expressed during biofilm development of methicillin resistant *Staphylococcus aureus* (MRSA). *Infect Genet Evol* 18: 106-112.
- Tuon FF, Dantas LR, Suss PH, Tasca Ribeiro VS. 2022. Pathogenesis of the *Pseudomonas aeruginosa* Biofilm: A Review. *Pathogens* 11(3): 300. <https://doi.org/10.3390/pathogens11030300>.
- Dai L, Wu TQ, Xiong YS, Ni HB, Ding Y, Zhang WC, ..., Yu J. 2019. Ibuprofen-mediated potential Inhibition of biofilm development and quorum sensing in *Pseudomonas aeruginosa*. *Life Sci* 237: 116947. <https://doi.org/10.1016/j.lfs.2019.116947>.
- Ha DG, O'Toole GA. 2015. C-di-GMP and its effects on biofilm formation and dispersion: a *Pseudomonas aeruginosa* review. *Microbiol Spectr* 3(2). <https://doi.org/10.1128/microbiolspec.MB-0003-2014>.
- Franklin MJ, Nivens DE, Weadge JT, Howell PL. 2011. Biosynthesis of the *Pseudomonas aeruginosa* extracellular polysaccharides, alginate, Pel, and Psl. *Front Microbiol* 2: 167. <https://doi.org/10.3389/fmicb.2011.00167>.
- Ma L, Conover M, Lu H, Parsek MR, Bayles K, Wozniak DJ. 2009. Assembly and development of the *Pseudomonas aeruginosa* biofilm matrix. *PLoS Pathog* 5(3): e1000354. <https://doi.org/10.1371/journal.ppat.1000354>
- Coulon C, Vinogradov E, Filloux A, Sadovskaya I. 2010. Chemical analysis of

- cellular and extracellular carbohydrates of a biofilm-forming strain *Pseudomonas aeruginosa* PA14. *PLoS One* 5(12): e14220. <https://doi.org/10.1371/journal.pone.0014220>.
- Dreier J, Ruggerone P. 2015. Interaction of antibacterial compounds with RND efflux pumps in *Pseudomonas aeruginosa*. *Front Microbiol* 6: 660. <https://doi.org/10.3389/fmicb.2015.00660>.
- Kazemi-Pasarvi S, Ebrahimi NG, Shahrampour D, Arab-Bafrani Z. 2020. Reducing cytotoxicity of poly (lactic acid) – based / zinc oxide nanocomposites while boosting their antibacterial activities by thymol for biomedical applications. *Int J Biol Macromol* 164: 4556-4565.
- Najafloo R, Behyari M, Imani R, Nour S. 2020. A mini-review of Thymol incorporated materials: Applications in antibacterial wound dressing. *J Drug Deliv Sci Technol* 60: 101904. <https://doi.org/10.1016/j.jddst.2020.101904>
- Nejabatdoust A, Zamani H, Salehzadeh A. 2019. Functionalization of ZnO nanoparticles by glutamic acid and conjugation with thiosemicarbazide alters expression of efflux pump genes in multiple drug-resistant *Staphylococcus aureus* strains. *Microb Drug Resist* 25(7): 966-974.
- Pfaffl MW. 2001. A new mathematical model for relative quantification in real-time RT-PCR. *Nucleic Acids Res* 29: e45. <https://doi.org/10.1093/nar/29.9.e45>.
- Foo KL, Hashim U, Muhammad K, Voon CH. 2014. Sol-gel synthesized zinc oxide nanorods and their structural and optical investigation for optoelectronic application. *Nanoscale Res Lett* 9(1): 1-10.
- Khan MF, Ansari AH, Hameedullah M, Ahmad E, Husain FM, Zia Q, ..., Aliev G. 2016. Sol-gel synthesis of thorn-like ZnO nanoparticles endorsing mechanical stirring effect and their antimicrobial activities: Potential role as nano-antibiotics. *Sci Rep* 6(1): 1-12.
- Sirelkhatim A, Mahmud S, Seeni A, Kaus NHM, Ann LC, Bakhori SKM, ..., Mohamad D. 2015. Review on zinc oxide nanoparticles: antibacterial activity and toxicity mechanism. *Nanomicro Lett* 7(3): 219-242.
- Li M, Zhu L, Lin D. 2011. Toxicity of ZnO nanoparticles to *Escherichia coli*: mechanism and the influence of medium components. *Environ Sci Technol* 45(5): 1977-1983.
- Tada R, Chavda N, Shah MK. 2011. Synthesis and characterization of some new thiosemicarbazide derivatives and their transition metal complexes. *J Chem Pharm Res* 3(2): 290-297.
- Yanishlieva NV, Marinova EM, Gordon MH, Raneva VG. 1999. Antioxidant activity and mechanism of action of thymol and carvacrol in two lipid systems. *Food Chem* 64(1): 59-66.
- Askoura M, Mottawea W, Abujamel T, Taher I. 2011. Efflux pump inhibitors (EPIs) as new antimicrobial agents against *Pseudomonas aeruginosa*. *Libyan J Med* 6: 5870. doi: 10.3402/ljm.v6i0.5870.